

Influence of surface reconstructions and epitaxial-growth conditions on long-range order in $\text{Si}_{1-x}\text{Ge}_x$ alloys

V. P. Kesan, F. K. LeGoues, and S. S. Iyer

IBM Research Division, Thomas J. Watson Research Center, Yorktown Heights, New York 10598

(Received 16 December 1991)

In this paper we show unambiguously that ordering in $\text{Si}_{1-x}\text{Ge}_x$ is an entirely kinetic phenomenon governed completely by growth conditions and surface reconstructions, and not by bulk thermodynamic equilibrium. We describe a set of experiments involving the use of annealing, surface modification through molecular-beam-epitaxial adlayers, ultrahigh-vacuum chemical vapor-deposition growth, and growth on Si substrates with different orientations which indicate that both low-temperature growth and a 2×1 reconstructed surface are individually necessary but not sufficient conditions to observe long-range order in $\text{Si}_{1-x}\text{Ge}_x$. The experimentally observed ordered phase, which consists of bilayers of Si and Ge along all four $\langle 111 \rangle$ directions, is a metastable phase that does not correspond to the lowest-energy phase of the alloy and is irreversibly destroyed by annealing. Our experiments also emphasize that ordering in $\text{Si}_{1-x}\text{Ge}_x$ occurs even in the absence of strain in $\text{Si}_{1-x}\text{Ge}_x$ films. Finally, we demonstrate that long-range order in $\text{Si}_{1-x}\text{Ge}_x$ occurs due to local segregation induced by stresses at the growing surface. This mechanism successfully explains all experimental findings to date.

I. INTRODUCTION

Atomic ordering has been studied extensively in metallic alloys and several elemental and compound semiconductor material systems.¹⁻³ Advances in heteroepitaxial growth techniques have permitted the observation of stable and metastable atomic arrangements which cannot be predicted from bulk phase diagrams at the same temperature range or composition.²⁻⁶ Ordering in elemental semiconductor alloys, such as $\text{Si}_{1-x}\text{Ge}_x$, has been observed by many workers,⁷⁻¹² and the presence of long-range order (LRO) has been attributed to strain in lattice-mismatched epitaxial SiGe layers, until it was shown that ordering exists in unstrained, bulklike SiGe films.¹⁰ This experimentally observed ordered phase does not correspond to the predicted lowest-energy phase of the $\text{Si}_{1-x}\text{Ge}_x$ alloy,⁴ consisting of alternating Si-Ge-Ge-Si layers along the $\langle 111 \rangle$ direction. Instead, the observed phase was shown to be a microscopically strained structure consisting of bilayers of Si and Ge along all four equivalent $\langle 111 \rangle$ directions.¹⁰ Further, this metastable ordered phase comes about by lateral site-specific segregation (i.e., preferential migration) of Si and Ge atoms, brought about by alternating tensile and compressive stresses in adjacent sites present on a 2×1 reconstructed Si(100) surface (see Fig. 1).^{11,13} This segregation, once established on the surface, is essentially frozen into the bulk, resulting in a metastable, ordered $\text{Si}_{1-x}\text{Ge}_x$ alloy.

In this paper, we show that epitaxial growth conditions, such as growth temperature and surface reconstructions at the growth front, directly determine the presence or absence of long-range order in $\text{Si}_{1-x}\text{Ge}_x$ alloy layers. Our experiments prove that long-range order in $\text{Si}_{1-x}\text{Ge}_x$ is a direct consequence of surface growth kinetics, and we compare our results with theoretical predictions in this material system.

II. EXPERIMENTAL TECHNIQUES

We have examined molecular-beam epitaxy (MBE) and ultrahigh-vacuum chemical-vapor deposition (UHV-CVD) $\text{Si}_{1-x}\text{Ge}_x$ ($0.1 \leq x \leq 0.8$) films grown on Si substrates with different orientation over a wide range of substrate temperature and growth conditions. Surface reconstructions occurring at the growth front were modified *in situ*, using an adlayer such as gallium, antimony, or boron, and monitored using low-energy electron diffraction (LEED). The presence or absence of order was determined using planar and cross-sectional transmission electron microscopy (TEM). The extent of impurity incorporation from the adlayer into the bulk SiGe film was determined by secondary-ion-mass spectroscopy (SIMS). In addition, the $\text{Si}_{1-x}\text{Ge}_x$ layers were annealed at different temperatures for varying amounts of time, to study the stability of the ordered SiGe phase.

III. RESULTS

A. Dependence of LRO on growth and annealing temperatures

$\text{Si}_{0.5}\text{Ge}_{0.5}$ films, 5000 Å thick, were grown on Si(100) substrates by MBE at growth temperatures between 390 and 590 °C. Figures 2(a)–2(c) show diffraction patterns from a planar-view sample taken along the (110) zone axis for three different growth temperatures: (a) 390, (b) 490, and (c) 590 °C. The diffraction pattern in Fig. 2(a) clearly shows the presence of additional superlattice reflections present at $\frac{1}{2}\{111\}$, indicating strong order in the sample. The same extra reflections persist in Fig. 2(b), but are considerably weakened in intensity. In Fig. 2(c), we can see from the overexposed diffraction that these spots have disappeared completely, indicating the

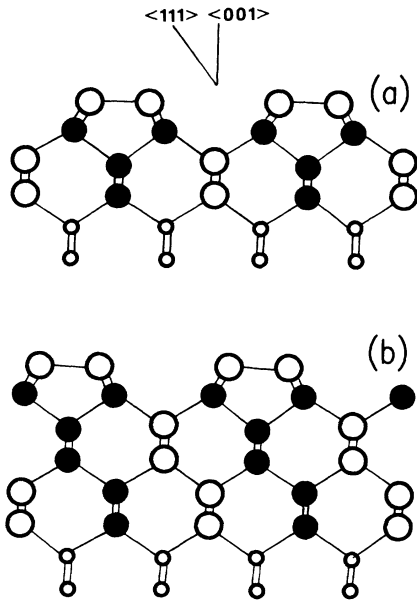


FIG. 1. (a) Cross section of the (100) 2×1 surface, projected onto a (110) plane. Surface dimers are at the top. Large solid circles correspond to sites under compressive stress, favoring Si occupancy. Large open circles denote sites under tensile stress, favoring Ge. (Dimer sites are also shown as large open circles, despite their small stress, because the surface energy favors Ge occupancy for those sites.) Small circles denote sites with little preference for Si or Ge. (b) Proposed growth process: The third and deeper layers in (a) are assumed immobile, while two more layers are added. Thus, the circles in the fifth and sixth layers denote Si or Ge occupancy, due only to kinetics (past history), rather than to actual stress or any equilibrium preference.

absence of long-range order in the $\text{Si}_{1-x}\text{Ge}_x$ films grown at high temperatures by MBE. It is important to note here that the complete absence of long-range order in the sample shown in Fig. 2(c) corresponds to no indication of either (SiGe)/(GeSi) type of order (referred to in the literature^{6,12} as rhombohedral structure 1, RH1) or (SiSi)/(GeGe) type of order (referred to in the literature^{6,12} as rhombohedral structure 2, RH2).

Ordered $\text{Si}_{1-x}\text{Ge}_x$ ($0.1 \leq x \leq 0.8$) films were annealed for 2 h at temperatures between 450 and 800 °C. Figure 3 shows the effect of annealing temperature on LRO in $\text{Si}_{1-x}\text{Ge}_x$ films as a function of Ge composition. Ordering in $\text{Si}_{0.5}\text{Ge}_{0.5}$ films persists up to annealing temperatures of 650 °C. However, $\text{Si}_{1-x}\text{Ge}_x$ films with Ge compositions either less than or greater than 50% are less stable to high-temperature annealing, and ordering is destroyed at temperatures around 500 °C. In addition, once ordering is destroyed, long-term annealing for several hours over a wide range of annealing temperatures fail to restore long-range order in either the RH2 or RH1 bilayer sequence.

Since ordering in $\text{Si}_{1-x}\text{Ge}_x$ is a strong function of temperature, it is important to establish the degree of long-range order that exists in these epitaxial $\text{Si}_{1-x}\text{Ge}_x$ films. We have used grazing angle x-ray diffraction and resonant Raman scattering to determine the extent of order-

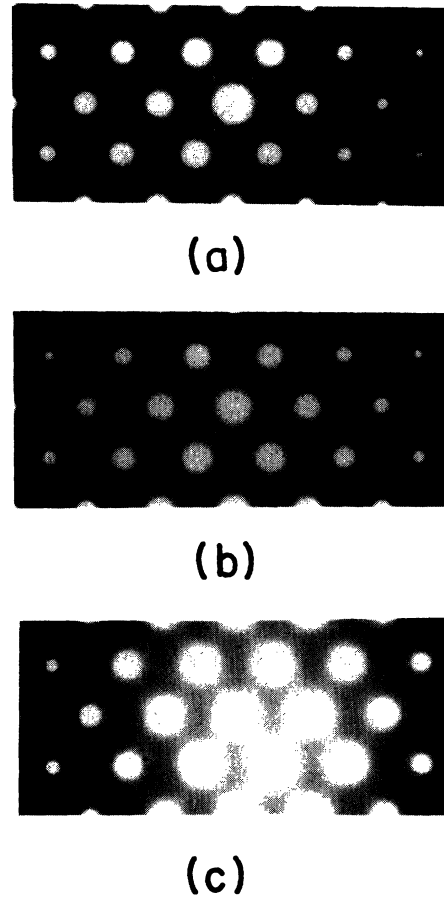


FIG. 2. Diffraction patterns from a planar-view sample taken along the (110) zone axis for three different growth temperatures, (a) 390, (b) 490, and (c) 590 °C. The diffraction pattern in (a) clearly shows the presence of additional superlattice reflections present at $\frac{1}{2}\{111\}$, indicating strong order in the sample. The same superlattice reflections persist in (b), but are considerably weakened in intensity. In (c), we can see from the overexposed diffraction that these spots have disappeared completely, indicating no order.

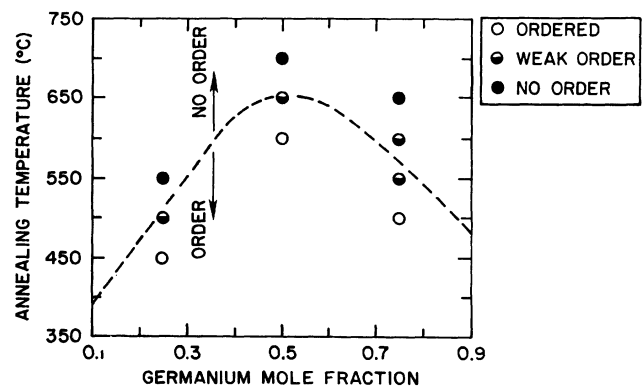


FIG. 3. Effect of annealing temperature on LRO in $\text{Si}_{1-x}\text{Ge}_x$ films as a function of Ge composition. Ordering in $\text{Si}_{0.5}\text{Ge}_{0.5}$ films persists up to annealing temperatures of 650 °C. However, $\text{Si}_{1-x}\text{Ge}_x$ films with Ge compositions either less than or greater than 50% are less stable to high-temperature annealing, and ordering is destroyed (absence of both RH1 and RH2 structures) at temperatures around 500 °C.

ing in $\text{Si}_{0.5}\text{Ge}_{0.5}$ layers grown at 390 and 490 °C. In other words, the relative proportion of Si and Ge in their respective bilayers was quantified. For a $\text{Si}_{0.5}\text{Ge}_{0.5}$ film grown at 390 °C, the ratio of the intensities of peaks at $\frac{1}{2}(777)$ and $\frac{1}{2}(888)$ in the x-ray-diffraction spectra was found to be 0.114. Taking into account the structure factor associated with the change in unit-cell parameters due to the strain induced by the presence of Ge, and the correcting factor related to the experiment geometry, we find the ordering parameter to be 0.64. Hence, the Si (or Ge) bilayers for a $\text{Si}_{0.5}\text{Ge}_{0.5}$ film are expected to contain about 18% Ge (or Si). The extent of ordering was also determined using resonant Raman scattering by comparing the relative strength of the Si-Si, Ge-Ge, and Si-Ge vibrations, and found to be around 70–80%.¹⁴ $\text{Si}_{0.5}\text{Ge}_{0.5}$ films grown at 490 °C showed 50% weaker ordering by x-ray diffraction compared to films grown at 390 °C, consistent with the electron-diffraction spectra seen in Fig. 2.

B. Surface modification

The nature of the reconstructed Si surface during growth plays a determining role in the ordering of $\text{Si}_{1-x}\text{Ge}_x$ films. Surface reconstruction on a Si(100) substrate were modified *in situ* during growth using antimony, gallium, and boron, and their effect on LRO was examined. Initially, a 5000-Å-thick, $\text{Si}_{0.5}\text{Ge}_{0.5}$ film was grown on a normal 2×1 reconstructed Si(100) substrate at low growth temperatures, to produce an ordered $\text{Si}_{0.5}\text{Ge}_{0.5}$ layer. Subsequently, the Si surface was saturated by 0.25–0.50 monolayer (ML) of antimony which causes the reconstruction on the Si(100) surface to change from a 2×1 to a 1×1 structure.^{15,16} The change in surface reconstruction was confirmed by *in situ* LEED of the quenched growth surface. $\text{Si}_{0.5}\text{Ge}_{0.5}$ growth was initiated again on the 1×1 reconstructed surfaces while continuing to maintain antimony coverage to ensure a 1×1 LEED pattern at the growth front. Figure 4 shows the cross section of this sample with a 5000-Å-thick, SiGe bottom layer followed by another 5000 Å of SiGe grown

on a 1×1 reconstructed surface. Also shown in Fig. 4 are the corresponding electron-diffraction patterns, together with the *in situ* LEED patterns, to elucidate the two different growth conditions. The electron-diffraction patterns in Fig. 4 clearly show that the bottom $\text{Si}_{0.5}\text{Ge}_{0.5}$ layer is strongly ordered, while the top $\text{Si}_{0.5}\text{Ge}_{0.5}$ layer is not.

Saturation of the growth surface with gallium instead of antimony gives similar, if somewhat less striking, results. Figure 5 shows a cross-sectional view of a 1.0- μm $\text{Si}_{0.5}\text{Ge}_{0.5}$ film where the top 5000 Å was grown under conditions to sustain a 0.25–0.50 monolayer of gallium at the growing surface. We can see from the electron-diffraction pattern in Fig. 5 that the bottom 5000 Å is strongly ordered, and the LEED pattern taken during the growth of this layer shows a distinct 2×1 structure at the growth front. The surface was then dosed with gallium, which caused the surface reconstruction to change to a weak 2×1 or a disordered 1×1 structure. Any additional gallium coverage immediately caused gallium precipitation on the SiGe surface, and it is thus difficult to maintain a good 1×1 reconstruction during growth. The next 5000 Å of $\text{Si}_{0.5}\text{Ge}_{0.5}$ was grown by maintaining the resulting 1×1 structure at the growth front. The electron-diffraction pattern corresponding to this layer (this pattern has been overexposed in order to determine the presence of additional superlattice reflections) in Fig. 5 shows a very weak ordering in the $\text{Si}_{0.5}\text{Ge}_{0.5}$ film.

The effect of doping with boron is drastically different since the growth surface retains a 2×1 reconstruction (i.e., there is no adlayer) in the presence of a boron flux. Figure 6 shows a cross-sectional view and diffraction pattern of a boron-doped $\text{Si}_{0.5}\text{Ge}_{0.5}$ film. The structure in Fig. 6 corresponds to a Si/ $\text{Si}_{0.5}\text{Ge}_{0.5}$ resonant tunneling structure, but in our discussions only the 1.0- μm -thick $\text{Si}_{0.5}\text{Ge}_{0.5}$ layer is relevant. The electron-diffraction pattern in Fig. 6 clearly shows that the boron-doped $\text{Si}_{0.5}\text{Ge}_{0.5}$ film is strongly ordered.

We have also examined $\text{Si}_{1-x}\text{Ge}_x$ films grown by UHV-CVD at 560 and 450 °C. The SiGe films grown at

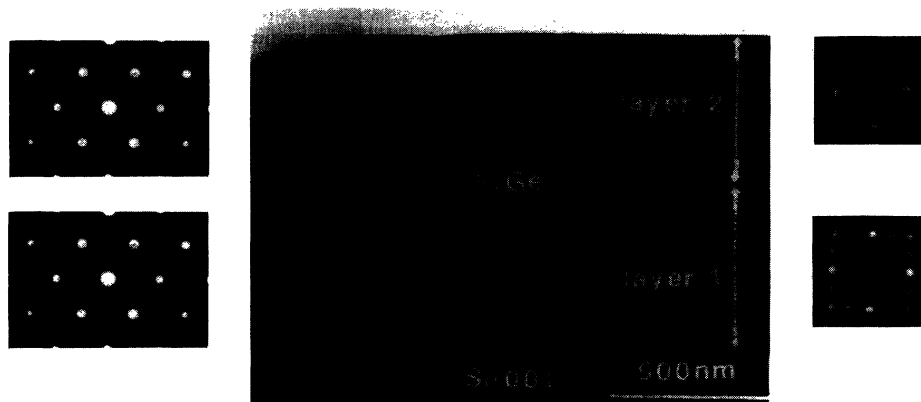


FIG. 4. Cross-sectional view of a sample with a 5000-Å-thick $\text{Si}_{0.5}\text{Ge}_{0.5}$ layer, followed by another 5000 Å of $\text{Si}_{0.5}\text{Ge}_{0.5}$, grown with Sb coverage on a 1×1 reconstructed surface. Also shown are the corresponding electron-diffraction patterns, together with the *in situ* LEED patterns, to elucidate the two different growth conditions. The electron-diffraction patterns clearly show that the bottom $\text{Si}_{0.5}\text{Ge}_{0.5}$ layer is strongly ordered, while the top $\text{Si}_{0.5}\text{Ge}_{0.5}$ layer is not.

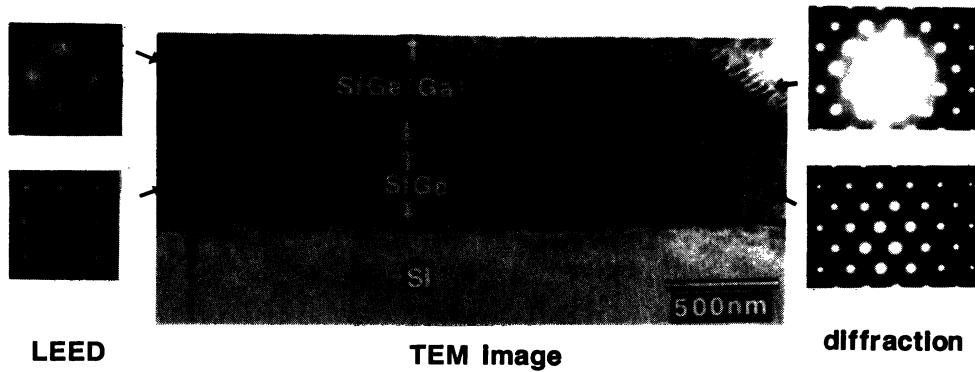


FIG. 5. Cross-sectional view of a 1.0- μm $\text{Si}_{0.5}\text{Ge}_{0.5}$ film, where the top 5000 \AA was grown under conditions to sustain 0.25–0.50 monolayer of gallium at the growing surface. Also shown are the corresponding electron-diffraction patterns, together with the *in situ* LEED patterns, to elucidate the two different growth conditions. The electron-diffraction patterns clearly show that the bottom $\text{Si}_{0.5}\text{Ge}_{0.5}$ layer is strongly ordered, while the top $\text{Si}_{0.5}\text{Ge}_{0.5}$ layer is very weakly ordered.

low temperatures (450 $^{\circ}\text{C}$) by UHV-CVD are not ordered, but films grown at 560 $^{\circ}\text{C}$ are ordered. Due to intrinsic differences in MBE and CVD growth techniques, we find that the range of growth temperatures that produce ordered $\text{Si}_{1-x}\text{Ge}_x$ films in the two cases is distinctly different and actually the inverse of each other.

We have also examined $\text{Si}_{1-x}\text{Ge}_x$ films grown on Si substrates with different orientations. $\text{Si}_{1-x}\text{Ge}_x$ films

grown by MBE on Si(111) substrates do not show any ordering under the set of growth conditions that we have examined. In particular, the same growth temperatures that produce strong ordering in $\text{Si}_{1-x}\text{Ge}_x$ films grown on Si(100) substrates do not result in LRO when grown on Si(111) substrates. No amount of annealing of $\text{Si}_{1-x}\text{Ge}_x$ films grown on Si(111) substrates produce long-range order.

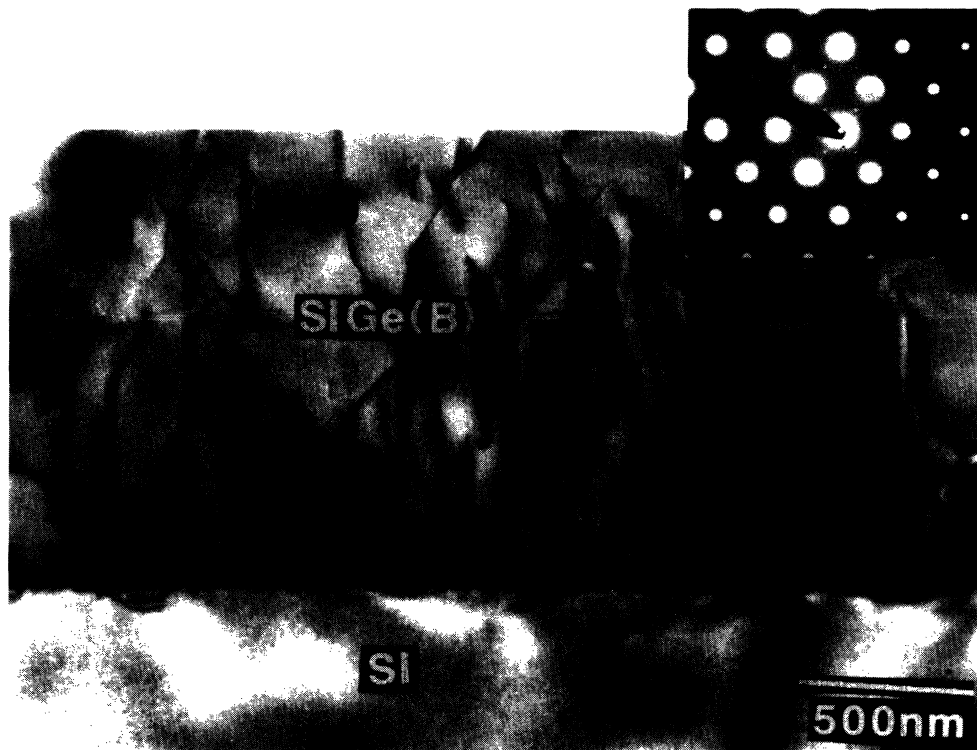


FIG. 6. A cross-sectional view and diffraction pattern of a boron-doped $\text{Si}_{0.5}\text{Ge}_{0.5}$ film. This structure corresponds to a $\text{Si}/\text{Si}_{0.5}\text{Ge}_{0.5}$ resonant tunneling structure, but in our discussions only the 1.0- μm -thick $\text{Si}_{0.5}\text{Ge}_{0.5}$ layer is relevant. The electron-diffraction pattern clearly shows that the boron-doped $\text{Si}_{0.5}\text{Ge}_{0.5}$ film is strongly ordered.

IV. DISCUSSION

A cross section of a Si(100) 2×1 reconstructed dimer structure [see Fig. 1(a)] shows that alternating atomic sites in the third and fourth layers of the film are under compressive or tensile stress.^{11,13} These atomic-scale stresses can cause site-specific segregation of Si and Ge atoms in the $\text{Si}_{1-x}\text{Ge}_x$ alloy, since sites under compressive stress would rather be occupied by the smaller silicon atom while those under tensile stress would be favored by the larger germanium atom. When a double layer is grown on the initial surface shown in Fig. 1(a), alternating Si-rich and Ge-rich pairs of atoms in the third and fourth layers of the crystal are seen again [see Fig. 1(b)]. At low growth temperatures, it is possible to "freeze in" this structure, because bulk diffusion coefficients are sufficiently low, and thus elemental distributions seen in the subspace layers are sustained throughout the epitaxial SiGe film. This mechanism results in the experimentally observed Si-Si-Ge-Ge-ordered phase, RH2 (see Fig. 1),¹⁰ and not the Si-Ge-Ge-Si phase, RH1, predicted by theory at very low temperatures. Recently, Jesson and Pennycook¹⁷ have proposed another kinetic growth model involving an asymmetric Ge-atom pump mechanism to explain Ge segregation and the ordering in ultrathin Si-Ge superlattices that then arises from it. In the following discussion, we will show that all experimental results described in the preceding section are consistent with the mechanism proposed in Fig. 1.

The fact that once ordering in $\text{Si}_{1-x}\text{Ge}_x$ is annihilated by either annealing or high-temperature growth it cannot be restored by subsequent long-term annealing clearly indicates that the ordered phase of the $\text{Si}_{1-x}\text{Ge}_x$ alloy is a metastable phase which occurs under certain epitaxial growth conditions. Ordering in $\text{Si}_{0.5}\text{Ge}_{0.5}$ persists at higher annealing temperatures than in $\text{Si}_{1-x}\text{Ge}_x$ films with unequal percentages of Si and Ge (see Fig. 3). This is consistent with the fact that fewer atomic displacements are necessary to cause destruction of long-range order in $\text{Si}_{1-x}\text{Ge}_x$ films with unequal amounts of Si and Ge.

It is clear from the adlayer surface modification experiments that simply changing the surface reconstruction from a 2×1 to a 1×1 *in situ* during growth alters the phase of the SiGe alloy and unambiguously demonstrates that ordering is entirely due to surface kinetics. It is important to rule out any extensive incorporation from the adlayer species into the SiGe film which might result in a change in the bulk properties of the alloy. Figure 7 shows a SIMS profile of the sample described in Fig. 4, and the extent of bulk antimony incorporation into the top $\text{Si}_{0.5}\text{Ge}_{0.5}$ layer from the antimony adlayer at the growth front is around $2\times 10^{20}/\text{cm}^3$. Antimony-implanted $\text{Si}_{0.5}\text{Ge}_{0.5}$ films were used as standards to calibrate the SIMS profiles. This amount of antimony incorporation ($< 0.5\%$) into the $\text{Si}_{0.5}\text{Ge}_{0.5}$ is sufficiently low as not to have any effect on the bulk phase stability of this layer.

A weak 2×1 LEED pattern is observed during the growth of $\text{Si}_{0.5}\text{Ge}_{0.5}$ films saturated with a gallium adlayer, and this results in a weakly ordered $\text{Si}_{0.5}\text{Ge}_{0.5}$ film.

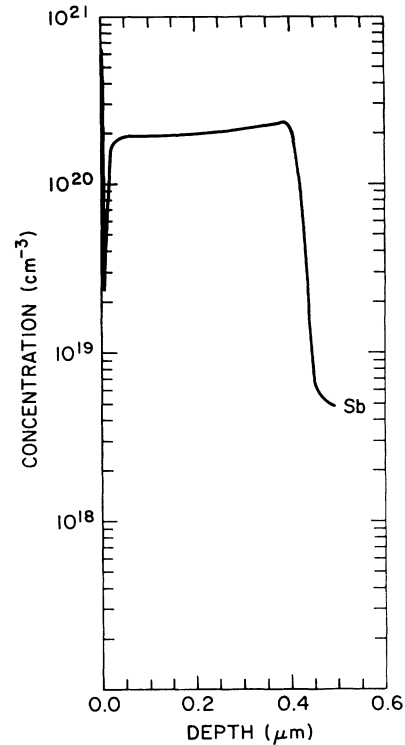


FIG. 7. SIMS profile of antimony in the $\text{Si}_{0.5}\text{Ge}_{0.5}$ sample described in Fig. 4. The extent of bulk antimony incorporation into the top $\text{Si}_{0.5}\text{Ge}_{0.5}$ layer from the antimony adlayer at the growth front is around $2\times 10^{20}/\text{cm}^3$ ($< 0.5\%$).

The use of gallium adlayers results in an intermediate set of results between antimony and boron, which show that dynamic changes in the 2×1 reconstruction directly impact the extent of ordering in the SiGe layer. This reinforces the important role played by the atomic arrangement at the growing surface on ordering in the bulk $\text{Si}_{1-x}\text{Ge}_x$. Figure 8 shows a SIMS profile of gallium in the $\text{Si}_{0.5}\text{Ge}_{0.5}$ sample described in Fig. 5, and the amount of gallium incorporated in the film is again sufficiently low ($< 0.15\%$) as to not cause any bulk change in the $\text{Si}_{0.5}\text{Ge}_{0.5}$.

Boron, which is a *p*-type dopant in Si and $\text{Si}_{1-x}\text{Ge}_x$, incorporates readily into the bulk, and does not result in a change in the surface reconstruction at the growth front. Hence, a 2×1 structure can be maintained at the Si(100) surface while exposing the $\text{Si}_{0.5}\text{Ge}_{0.5}$ surface to a boron flux, and this produces a highly ordered $\text{Si}_{0.5}\text{Ge}_{0.5}$ film.

$\text{Si}_{1-x}\text{Ge}_x$ films grown by UHV-CVD permit one to examine the effect of surface reconstruction on LRO without the use of adlayers. This is because in the UHV-CVD environment, at low growth temperatures, there is significant hydrogen coverage and the Si(100) surface is 1×1 reconstructed.^{18,19} At higher growth temperatures, around 550°C , the hydrogen coverage is less complete, and a 2×1 reconstructed Si surface is seen. Indeed, in keeping with our previous observations, we find that UHV-CVD SiGe films grown at higher temperatures are ordered, but those grown at lower temperatures are not.

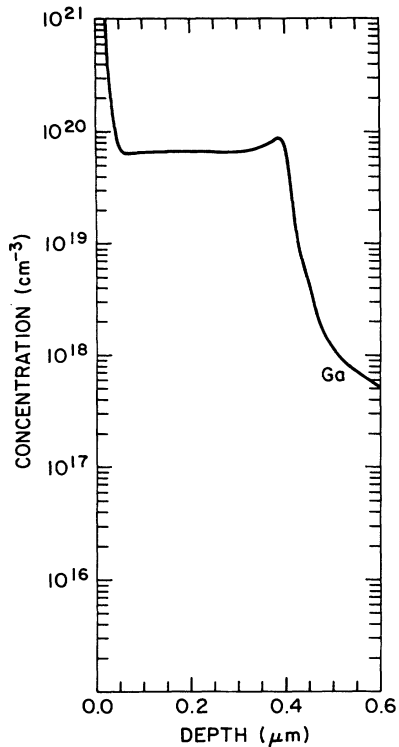


FIG. 8. SIMS profile of gallium in the $\text{Si}_{0.5}\text{Ge}_{0.5}$ sample described in Fig. 5. The amount of gallium incorporated in the film is again sufficiently low ($< 0.15\%$) as to not cause any bulk change in the $\text{Si}_{0.5}\text{Ge}_{0.5}$.

While this is seemingly contradictory with the MBE-grown SiGe results, a closer examination of the conditions which produce LRO in both MBE and UHV-CVD films indicates that *both* conditions relating to low-temperature growth and a 2×1 surface reconstruction must be maintained to observe LRO.

Growth on Si(111) substrates allows one to examine $\text{Si}_{1-x}\text{Ge}_x$ films grown on a 7×7 reconstructed Si surface. These $\text{Si}_{1-x}\text{Ge}_x$ films show no ordering under any set of growth or annealing conditions. This once again indicates that a 2×1 reconstructed surface is necessary to see LRO.

The extent of long-range order in the $\text{Si}_{1-x}\text{Ge}_x$ films, and the range of temperature for which ordering is strong enough to be detected, is significantly higher than that predicted by Kelires and Tersoff.¹³ It is difficult to gauge how accurately stress at the growing surface can be described by the empirical classical potential used in their model. Further, since their model refers to thermodynamic equilibrium only, this discrepancy is not surprising.

V. CONCLUSION

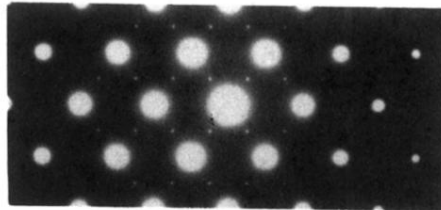
In conclusion, we show unambiguously that ordering in $\text{Si}_{1-x}\text{Ge}_x$ is an entirely kinetic phenomenon, governed completely by growth conditions and surface reconstructions, and not by bulk thermodynamic equilibrium as was previously believed. The experimentally observed ordered phase, which consists of bilayers of Si and Ge along all four $\langle 111 \rangle$ directions, is a metastable phase that does not correspond to the lowest-energy phase of the alloy, and is irreversibly destroyed by annealing. The set of experiments described in this paper involving the use of annealing, surface modification through adlayers, UHV-CVD growth, and growth on Si(111) substrates, all indicate that both low-temperature growth and a 2×1 reconstructed surface are individually necessary but not sufficient to observe LRO in $\text{Si}_{1-x}\text{Ge}_x$. Our experiments also emphasize that ordering in $\text{Si}_{1-x}\text{Ge}_x$ occurs in the absence of strain, and indeed $\text{Si}/\text{Si}_{1-x}\text{Ge}_x$ strained-layer superlattices grown on Si substrates with different orientations show no order.²⁰ We have also ruled out previous explanations of ordering in $\text{Si}_{1-x}\text{Ge}_x$, and proposed a mechanism that ordering in $\text{Si}_{1-x}\text{Ge}_x$ is related with local segregation induced by stresses at the surface, and successfully explained all experimental findings to date.

ACKNOWLEDGMENTS

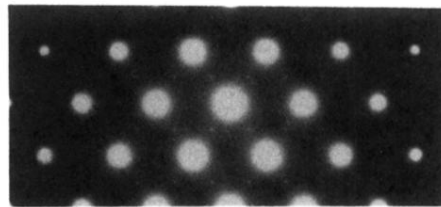
We would like to acknowledge the technical assistance of B. A. Ek and R. Griffin, B. S. Meyerson for providing the UHV-CVD samples, A. Segmüller for the x-ray-diffraction analysis, and J. Tersoff for many useful discussions.

¹M. Hansen and K. Anderko, *Constitution of Binary Alloys* (McGraw-Hill, New York, 1958).
²T. S. Kuan, in *Encyclopedia of Physical Science and Technology*, edited by K. A. Meyers (Academic, New York, 1989), p. 521.
³M. A. Shahid, S. Mahajan, D. E. Laughlin, and H. M. Cox, *Phys. Rev. Lett.* **58**, 2567 (1987).
⁴J. L. Martins and A. Zunger, *Phys. Rev. Lett.* **56**, 1400 (1986).
⁵C. P. Flynn, *Phys. Rev. Lett.* **57**, 599 (1986).
⁶J. E. Bernard and A. Zunger, *Phys. Rev. B* **44**, 1663 (1991).
⁷A. Ourmazd and J. C. Bean, *Phys. Rev. Lett.* **55**, 765 (1985).
⁸D. J. Lockwood, K. Rajan, E. W. Fenton, J.-M. Baribeau, and M. W. Denhoff, *Solid State Commun.* **61**, 465 (1987).
⁹E. Müller, H.-U. Nissen, M. Ospelt, and H. von Känel, *Phys. Rev. Lett.* **63**, 1819 (1989).
¹⁰F. K. LeGoues, V. P. Kesan, and S. S. Iyer, *Phys. Rev. Lett.* **64**, 40 (1990).

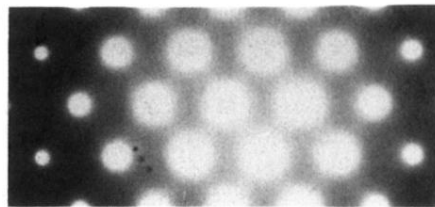
¹¹F. K. LeGoues, V. P. Kesan, S. S. Iyer, J. Tersoff, and R. Tromp, *Phys. Rev. Lett.* **64**, 2038 (1990).
¹²E. Müller, H.-U. Nissen, K. A. Mader, M. Ospelt, and H. von Känel, *Philos. Mag. Lett.* **64**, 183 (1991).
¹³P. C. Kelires and J. Tersoff, *Phys. Rev. Lett.* **63**, 1164 (1989).
¹⁴J. C. Tsang, V. P. Kesan, J. L. Freeouf, F. K. LeGoues, and S. S. Iyer (unpublished).
¹⁵R. A. Metzger and F. G. Allen, *Surf. Sci.* **137**, 397 (1984).
¹⁶R. A. Metzger and F. G. Allen, *J. Appl. Phys.* **55**, 931 (1984).
¹⁷D. E. Jesson, S. J. Pennycook, and J.-M. Baribeau, *Phys. Rev. Lett.* **66**, 750 (1991).
¹⁸M. Liehr, C. M. Greenlief, S. R. Kasi, and M. Offenber, *Appl. Phys. Lett.* **56**, 629 (1990).
¹⁹S. S. Iyer, M. Arienzo, and E. de Frésart, *Appl. Phys. Lett.* **57**, 893 (1990).
²⁰T. S. Kuan and S. S. Iyer, *Appl. Phys. Lett.* **59**, 2242 (1991).



(a)



(b)



(c)

FIG. 2. Diffraction patterns from a planar-view sample taken along the (110) zone axis for three different growth temperatures, (a) 390, (b) 490, and (c) 590°C. The diffraction pattern in (a) clearly shows the presence of additional superlattice reflections present at $\frac{1}{2}\{111\}$, indicating strong order in the sample. The same superlattice reflections persist in (b), but are considerably weakened in intensity. In (c), we can see from the overexposed diffraction that these spots have disappeared completely, indicating no order.

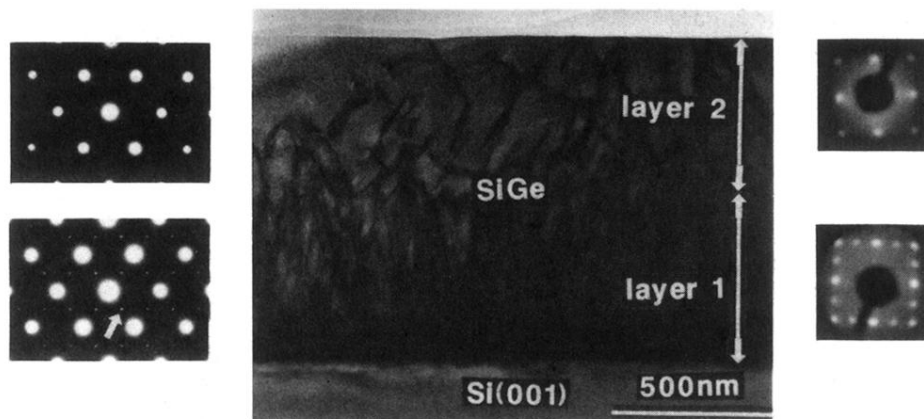


FIG. 4. Cross-sectional view of a sample with a 5000-Å-thick $\text{Si}_{0.5}\text{Ge}_{0.5}$ layer, followed by another 5000 Å of $\text{Se}_{0.5}\text{Ge}_{0.5}$, grown with Sb coverage on a 1×1 reconstructed surface. Also shown are the corresponding electron-diffraction patterns, together with the *in situ* LEED patterns, to elucidate the two different growth conditions. The electron-diffraction patterns clearly show that the bottom $\text{Si}_{0.5}\text{Ge}_{0.5}$ layer is strongly ordered, while the top $\text{Si}_{0.5}\text{Ge}_{0.5}$ layer is not.

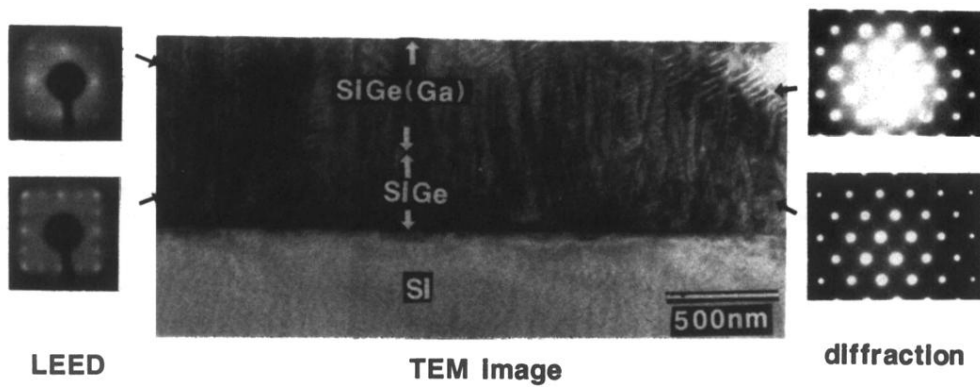


FIG. 5. Cross-sectional view of a $1.0\text{-}\mu\text{m}$ $\text{Si}_{0.5}\text{Ge}_{0.5}$ film, where the top 5000 \AA was grown under conditions to sustain $0.25\text{--}0.50$ monolayer of gallium at the growing surface. Also shown are the corresponding electron-diffraction patterns, together with the *in situ* LEED patterns, to elucidate the two different growth conditions. The electron-diffraction patterns clearly show that the bottom $\text{Si}_{0.5}\text{Ge}_{0.5}$ layer is strongly ordered, while the top $\text{Si}_{0.5}\text{Ge}_{0.5}$ layer is very weakly ordered.

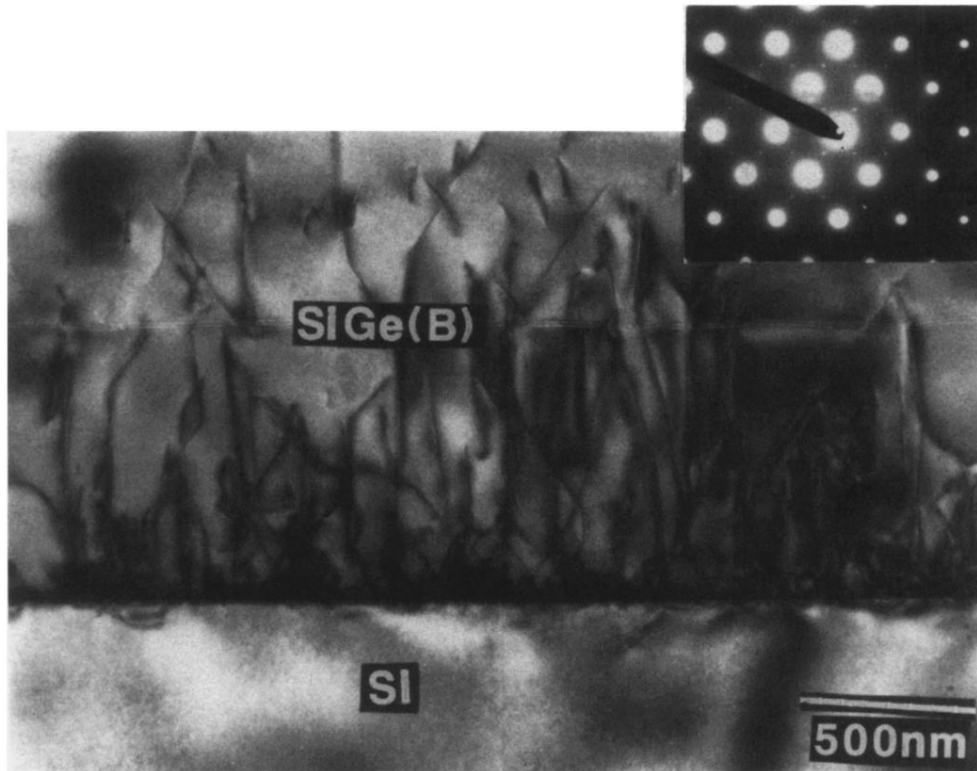


FIG. 6. A cross-sectional view and diffraction pattern of a boron-doped $\text{Si}_{0.5}\text{Ge}_{0.5}$ film. This structure corresponds to a $\text{Si}/\text{Si}_{0.5}\text{Ge}_{0.5}$ resonant tunneling structure, but in our discussions only the $1.0\text{-}\mu\text{m}$ -thick $\text{Si}_{0.5}\text{Ge}_{0.5}$ layer is relevant. The electron-diffraction pattern clearly shows that the boron-doped $\text{Si}_{0.5}\text{Ge}_{0.5}$ film is strongly ordered.